

# IMPEDANCE MEASUREMENTS, COMPUTATIONS AND THEIR INTERPRETATION

A. Hofmann, CERN, Geneva, Switzerland

## Abstract

The impedance represented by the beam surroundings leads to collective effects which limit the intensity of an accelerator. The components seen by the beam are designed for a small impedance with the help of computer codes and of laboratory measurements on models. Once the machine is built different collective effects are measured. The observed parasitic mode loss, bunch lengthening and frequency shifts of the incoherent and the quadrupole mode synchrotron oscillation give integrals over the longitudinal resistive and reactive impedances. Growth or decay rates of head-tail modes and betatron frequency shifts give corresponding information for the transverse impedance. Observing the current dependence of the orbit and of the betatron phase advances around the ring can localize the impedance and distinguish between the different contributions. Coupled bunch mode instabilities are usually driven by a single, narrow band resonance and their behavior can help to identify the responsible parasitic mode in the cavities. For unbunched beams the oscillating mode gives directly the frequency of the driving resonator. The beam transfer function is a powerful tool to determine the impedance at low frequencies. From a set of observed collective effects a model of the impedance is obtained which can be compared with expectations.

## 1 INTRODUCTION

The impedance is the voltage induced by a frequency component of the beam current. The impedance is a function of the geometry and the electric properties of the beam surroundings and the frequency. It refers to an ultra-relativistic case and is independent of the beam properties.

To introduce the impedance we consider a cavity like object, shown in Fig. 1, which resembles an  $RLC$ -circuit having a shunt impedance  $R_s$ , a capacity  $C$  and an inductance  $L$ . We replace these quantities with parameters which can easily be measured or calculated: the resonant frequency  $\omega_r = 1/\sqrt{LC}$ , the quality factor  $Q = R_s\sqrt{C/L} = R_s/(\omega_r L)$  and the damping rate  $\alpha_r = \omega_r/(2Q)$ .

The voltage  $V$  induced by a current  $I$  is given by the differential equation

$$\ddot{V} + \frac{\omega_r}{Q}\dot{V} + \omega_r^2 V = \frac{\omega_r R_s}{Q}\dot{I}. \quad (1)$$

We take first the case in which the cavity is excited by a delta function current pulse, or a short bunch  $I(t) = q\delta(t)$ .

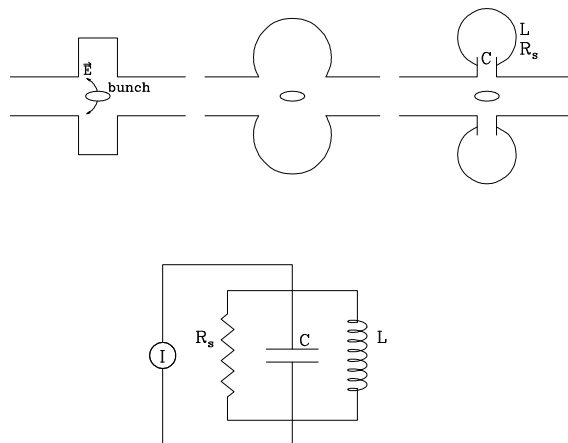


Figure 1:  $RLC$ -circuit equivalent to a cavity resonance

The resulting voltage is

$$V(t) = 2qk e^{-\alpha_r t} \left( \cos(\omega_r^* t) - \frac{\omega_r \sin(\omega_r^* t)}{2Q\omega_r^*} \right) = qG(t), \quad (2)$$

where we use the parasitic mode loss factor  $k$

$$k = \frac{\omega_r R_s}{2Q} \text{ and } \omega_r^* = \omega_r \sqrt{1 - \frac{1}{4Q^2}}. \quad (3)$$

This voltage is induced by a point charge  $q$  going through the cavity at the time  $t = 0$ . A second point charge  $q'$  passing through the cavity at a later time  $t$  loses the energy  $U = q'V(t)$ . This energy gain/loss per unit source and probe charge is called the wake potential of a point charge or also the **Green function**  $G(t)$ . It vanishes for negative values of  $t$  since we assumed an ultra-relativistic case  $\beta \rightarrow 1$  where no field is present before the charge arrives.

The cavity can also be excited by a harmonic current

$$I(t) = \hat{I} e^{j\omega t} \text{ with } -\infty \leq \omega \leq \infty. \quad (4)$$

The induced voltage divided by this current is called the impedance at the frequency  $\omega$

$$Z(\omega) = R_s \frac{1 + jQ \frac{\omega_r^2 - \omega^2}{\omega_r \omega}}{1 + Q^2 \left( \frac{\omega^2 - \omega_r^2}{\omega_r \omega} \right)^2} = Z_r(\omega) + jZ_i(\omega). \quad (5)$$

It has a real and imaginary part, also called resistive and reactive part. At the resonant frequency  $\omega_r$ ,  $Z_r(\omega_r)$  has a

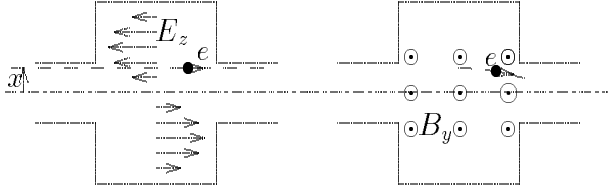


Figure 2: Transverse mode during excitation and deflection

maximum and  $Z_i(\omega_r) = 0$ , The latter is inductive below  $\omega_r$  and capacitive above.

The impedance can be generalized to other types than resonators keeping some of the properties, like the symmetry behavior

$$Z_r(\omega) = Z_r(-\omega) , Z_i(\omega) = -Z_i(-\omega), \quad (6)$$

the values at vanishing frequency

$$Z_r(0) = Z_i(0) = 0. \quad (7)$$

and the relation to the Green function by the Fourier transform

$$Z(\omega) = \int_{-\infty}^{\infty} G(t)e^{-j\omega t} dt = \int_0^{\infty} G(t)e^{-j\omega t} dt. \quad (8)$$

So far we investigated the **longitudinal impedance** in which the beam induces a longitudinal field leading to an energy change of the particle. There are also deflecting modes excited in the cavity which produce a transverse force, described by the **transverse impedance**. It is illustrated in Fig. 2 for a simple mode. Close to the axis it has at a certain time a longitudinal field with a transverse gradient. A quarter of an oscillation period later this field is transformed into a transverse magnetic field which can deflect a particle traversing the cavity at this time. It is important to observe that the mode is driven by the longitudinal motion of a beam going through the cavity at a transverse distance  $x$  from the axis and not by the transverse beam motion.

For a general mode the transverse impedance is defined as the ratio between the transverse force, integrated over the circumference or a particular element, and the dipole moment of the driving current at a given frequency  $\omega$ .

$$Z_{\perp}(\omega) = j \frac{\int_0^{2\pi R} [\vec{E}(\omega) + [\vec{\beta}c \times \vec{B}(\omega)]]_{\perp} ds}{I_y(\omega)}. \quad (9)$$

The factor  $j$  in front indicates that the deflecting force and the driving current dipole moment are out of phase.

## 2 CALCULATION OF IMPEDANCES

Most of the impedances in a ring have to be calculated numerically. One of the rare cases having an analytic expression is the resistive wall of a circular chamber with radius  $b$ ,

conductivity  $\kappa$  and permeability  $\mu = 1$  in a ring of average radius  $R$  [1]

$$Z(\omega) = (1 + j) \frac{\mu_0 R}{b} \sqrt{\frac{\omega}{2\mu_0 \kappa}} = (1 + j) \frac{\mu_0 R \delta \omega}{2b}, \quad (10)$$

where  $\delta$  is the skin depth  $\delta = \sqrt{2/(\mu_0 \kappa \omega)}$ .

The transverse impedance of this smooth resistive wall is

$$Z_{\perp}(\omega) = (1 + j) \frac{c\mu_0 R \delta}{b^3}. \quad (11)$$

Using the revolution frequency  $\omega_0 = R/c$  we can relate this transverse impedance to the longitudinal one

$$Z_{\perp}(\omega) = \frac{2R}{b^2} \frac{Z(\omega)}{\omega/\omega_0} = \frac{2R}{b^2} \frac{Z(\omega)}{n} \quad (12)$$

Most other impedances have to be computed. Several codes have been developed over the years which use basically two methods.

The first works in frequency domain and calculates modes of cavity-like objects giving their resonant frequencies  $\omega_r$  with the normalized shunt impedance  $R_s/Q$  and in most cases also with the quality factor  $Q$ . In this calculation the coupling of the mode to a beam traversing the object with the speed of light is considered and expressed by the so-called transit time factor. Such programs can also calculate deflecting modes and determine the corresponding transverse impedance.

Other codes work in time domain. They usually consider a Gaussian bunch of charge  $q$  and rms length  $\sigma$  traversing a cavity-like object and calculate the electromagnetic fields which satisfy the boundary condition. The program calculates the energy loss  $U$  of a test particle with charge  $q'$  traversing the cavity a time  $t$  after the bunch. Normalizing this with the charges of the source bunch and test particles gives the **wake potential**  $W(t, \sigma) = U/(qq')$  which becomes the Green function for vanishing bunch length.

The impedance usually has some resonances with narrow width, smaller than the revolution frequency  $\omega_0$  or the frequency  $M\omega_0$  of  $M$  bunches, created by parasitic modes in the RF-cavities. Since the fields excited in them decay slowly and are still present after one revolution or when the next bunch arrives they can drive coupled bunch instabilities. For single traversal effects only the area of these resonances and the broad band impedances are of importance.

Since it is impossible to measure the impedance in all details a broad band impedance model is often used to study and analyse single traversal effects. This model should have relatively simple expressions for the real and imaginary part of the impedance and for the Green function. Furthermore, the model should have vanishing impedance at zero frequency and satisfy the symmetry conditions. Often a broad band resonator is used and its resonant frequency, shunt impedance and quality factor adjusted to fit the measured or calculated impedances. At very high frequency the impedance can be obtained from diffraction effects of the

fields at aperture changes [2, 3, 4]. These diffraction calculations predicts that the impedance at very high frequency should scale like  $\omega^{-3/2}$  if the aperture changes are very regular like in a linac where the fields emitted at different irises can interfere, or, like  $\omega^{-1/2}$  if the aperture changes are less regular or have bends between them. In the latter case the energy loss of a bunch due to this impedance should scale like  $\omega^{-1/2}$  [5]. Obviously the broad band resonator model overestimates this impedance at high frequencies.

### 3 MEASURING NARROW BAND IMPEDANCES WITH THE BEAM

#### 3.1 Narrow band impedance from coupled bunch oscillations

Coupled bunch instabilities are driven by narrow band resonances. Usually there is one strong resonance being responsible for this and the aim of the experiments is to determine its properties, find it and damp it. A set of  $M$  equidistant bunches can oscillate in different longitudinal modes. First, there are the bunch shape modes  $m$  ( $m = 1$ : dipole,  $m = 2$ : quadrupole mode, etc) oscillating with  $m$  times the synchrotron frequency  $\omega_s$ . They produce an envelope spectra covering higher frequencies the larger  $m$  is.

The coupled bunch motion is described by the relative phase  $\Delta\phi$  between the oscillations of adjacent bunches and labeled by the coupled mode number  $n = M\Delta\phi/2\pi$ . Each such mode produces a spectrum with two synchrotron side bands within each band of  $M\omega_0$ . An impedance will produce an instability with a growth rate being proportional to the difference between the sums of its values at the upper and lower sidebands.

By observing a the bunch shape mode of an instability we can make a rough estimate of the frequency range of the narrow band impedance which is the cause. A quadrupole mode is driven by a higher frequency than a dipole mode. The coupled mode  $n$  can narrow down the frequency range but has some ambiguities since the coupled mode spectrum repeats every  $M\omega_0$ . Using a large number  $M$  of bunches can reduce this uncertainty. From the growth rate of the instability the shunt impedance can be estimated and by changing the bunch filling pattern an idea of quality factor of the resonance can be obtained.

Once the frequency of the driving impedance is determined we can find a list of candidates among the devices built into the ring. If they contain coupling loops - like most of the cavities - signals can sometimes be observed during the development of the instability [6, 7].

#### 3.2 Transfer function measurement with a continuous beam

Exciting a beam at a certain frequency and observing its response in amplitude, called **beam transfer function**, can give valuable information about its stability. A polar plot of the inverse response gives the stability diagram of the beam.

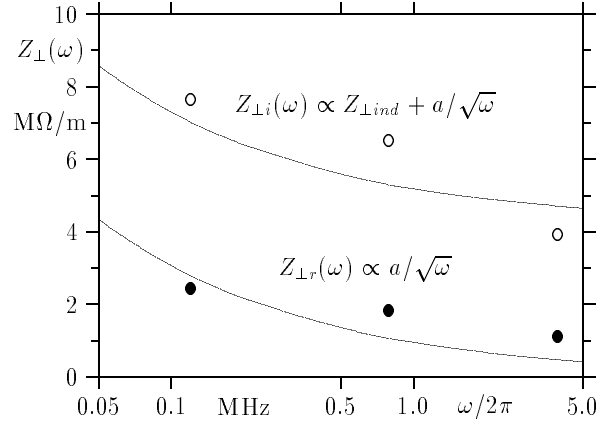


Figure 3: Measurement of  $Z_{\perp}$  at low frequencies using the transfer function on a continuous beam

The presence of a complex impedance shifts this diagram in a direction opposite to the impedance and by an amount proportional to the intensity, frequency spread, impedance and some other parameters. By changing one of these parameters by a known amount the diagram can be calibrated and the complex impedance determined. In Fig. 2 a measurement of the resistive and reactive impedance at low frequency obtained with this method is shown. In this range the smooth resistive wall is important and has been used to fit the results. For the reactive part the inductive tail of resonances of higher frequencies is still important and has been found to be  $Z_{\perp,ind} = 4.2$  M $\Omega$ /m by the fit of the results.

## 4 BROAD BAND LONGITUDINAL IMPEDANCE

#### 4.1 Resistive impedance from parasitic mode losses

An integral over the longitudinal resistive impedance times the power spectrum  $h(\omega)$  of the bunch is obtained by measuring the parasitic mode loss

$$U_{pm} = \frac{U}{eq} \propto \int Z_r(\omega) h(\omega) d\omega \quad (13)$$

Doing this for different bunch lengths this integral covers different frequency ranges which can be used to obtain to get some ideas of the frequency dependence of the impedance. The measurement is usually done filtering the beam signal at the RF-frequency and comparing its phase with the one of the RF-cavity voltage for different bunch currents.

We are often interested to measure the impedance at very high frequencies. This can be done with short electron bunches [8]. In an unbunched proton beam each particle produces at the wall a pulse which is due to the small opening angle of the field of length  $\sigma = (a/(\sqrt{2}\gamma))$ . By observing the slow energy loss of the beam due to this induced

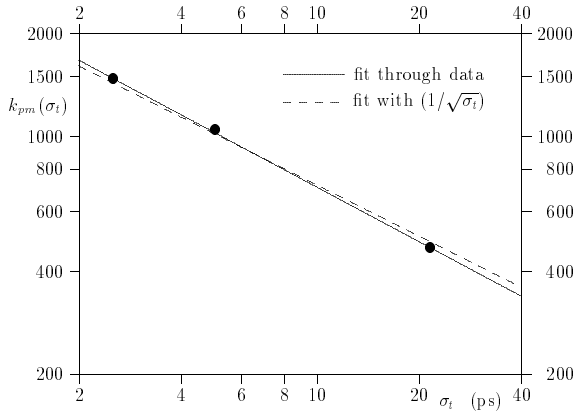


Figure 4: Parasitic mode loss obtained from the energy loss of a continuous proton beam

wall current we measure directly the parasitic mode loss factor  $k_{pm}(\sigma)$ . The result of such a measurement is shown in Fig. 4 which indicates that this factor decreases as  $1/\sqrt{\sigma}$  which is expected for an impedance having a  $1/\sqrt{\omega}$ -dependence at high frequencies.

In Fig. 5 the effect of the parasitic energy loss on the orbit is demonstrated. The effect results in a continuous decrease of this energy around the ring which results in a change of the local orbit at places of horizontal dispersion. In the passive cavity a strong local loss occurs. The energy is regained in the active cavity. The plotted measurement is just the difference between orbits measured at different bunch currents.

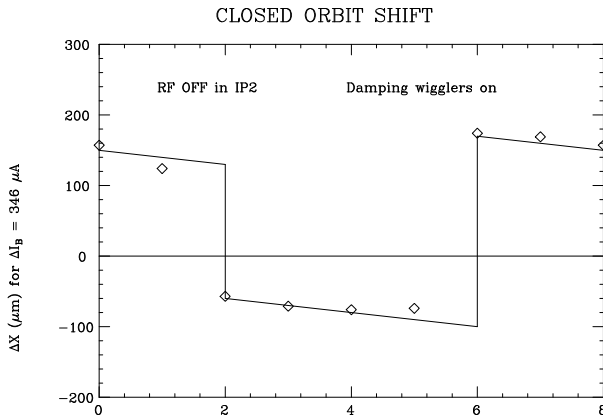


Figure 5: Difference orbits for 2 values of current giving the resistive impedance around the ring. In the experiment the RF-cavities at point 2 were not powered and only the ones in point 6 were operating

#### 4.2 Reactive impedance from synchrotron frequency shifts and bunch lengthening

In the reactive longitudinal impedance  $Z_i(\omega)$  the beam induces a voltage which changes the bunch length and the in-

coherent synchrotron frequency  $f_s$ . This effect is proportional to  $\int Z_i(\omega)h(\omega)d\omega$ . At relatively low frequencies the impedance is inductive leading to bunch lengthening. This bunch length can directly be measured. However, the incoherent synchrotron frequency is more difficult to observe. The coherent dipole mode frequency  $f_{s1}$  is not affected by this impedance since the oscillating bunch carries the wake potential with it. Usually the shift of the quadrupole mode frequency  $f_{s2}$  is observed.

## 5 BROAD BAND TRANSVERSE IMPEDANCE

### 5.1 Resistive impedance from the head-tail instability

A convenient way to obtain information about the resistive transverse impedance  $Z_{Ti}$  is the observation of the head-tail instability. Its growth rate is given proportional to  $\int Z_{\perp r}(\omega)h(\omega - \omega_\xi)d\omega$ . Here, the power spectrum of the bunch is shifted by the chromatic frequency  $\omega_\xi = Q'\omega_0/\eta$  with  $\eta = \alpha_c - 1/\gamma^2$ . For long bunches the impedance can be probed over a large frequency range by changing the chromaticity  $Q' = dQ/(dp/p)$ , [9].

### 5.2 The reactive impedance obtained from tune shifts with bunch current

The reactive impedance creates a shift of the coherent betatron frequencies which is proportional to  $\int Z_{\perp i}(\omega)h(\omega - \omega_\xi)d\omega$ . It is a very easy measurement to carry out since only the betatron frequencies have to be measured as a function of current. In Fig. 6 the results of such an experiment is shown in which not only the tunes but also the phase advances have been measured as a function of current. It shows localized strong change of the derivative  $d\mu/dI$  at the RF-cavities giving the same effect in both planes. In the arcs the effect is weaker and different for both planes due to the elliptic chamber.

## 6 SYNTHESIS OF THE IMPEDANCE MEASUREMENTS

With measurements done over different frequency ranges in the longitudinal and transverse planes one likes to summarize the results in an impedance model. It is in all practical cases impossible to cover all frequencies and some reasonable fit through the data has to be made. The impedance behavior at very low frequencies is often dominated by the smooth resistive wall. At intermediate frequencies some narrow band resonances are usually present. It is sufficient to know the strongest ones. These resonances become broader at about the cut-off frequency of the vacuum chamber. At very high frequencies the behavior is described by the diffraction model and a  $1/\sqrt{\omega}$ -behavior is expected. For single traversal effects a broad band resonator fit gives often a reasonable approximation except at the very high frequency end. This fit has the advantage the resistive and

imaginary parts have simple expressions and can be related to each other. Measurements of the two components can therefore be combined to determine the parameters of the model.

The transverse and longitudinal impedances have also some relation which can be used. For the resistive wall we found

$$Z_{\perp}(\omega) = \frac{2R}{b^2} \frac{Z(\omega)}{\omega/\omega_0} = \frac{2R}{b^2} \frac{Z(\omega)}{n} \quad (14)$$

For single resonances there is no such relations and they have different resonant frequencies in transverse and longitudinal cases. However, for the broad band impedances the above relation holds approximately and can be used to relate different measurements. If the chamber is not circular the transverse impedance in the two planes will be different.

The final impedance model can be used to calculate beam stability for different conditions. This can be helpful to optimize parameters like bunch length and filling pattern.

## 7 REFERENCES

- [1] V.K. Neil, A. Sessler; Rev. Sci. Instr., 36 (1965) p. 429.
- [2] A.M. Sessler; private note, 1969.
- [3] L.A. Vainstein; Soviet Phys. JETP 17 (1969) p. 709.
- [4] E. Keil; Nuclear Instr. and Methods 100 (1972) p. 419.
- [5] K. Bane and M. Sands; SLAC Pub 4441 (1987).
- [6] R.D. Kohaupt; IEEE Trans. on Nucl. Sci., NS-22 (1975) p. 1456.
- [7] D. Boussard et al.; IEEE Trans. on Nucl. Sci., NS-24 (1977) p. 1399.
- [8] R.F. Koontz, G.A. Loew, R.H. Miller; Proc. of the 8th Int. Conf. on High Energy Accel., CERN, Geneva (1971) p. 491.
- [9] J. Gareyte, F. Sacherer; Proc. of the 9th Int. Conf. on High Energy Accel., Stanford (1974) p. 341.

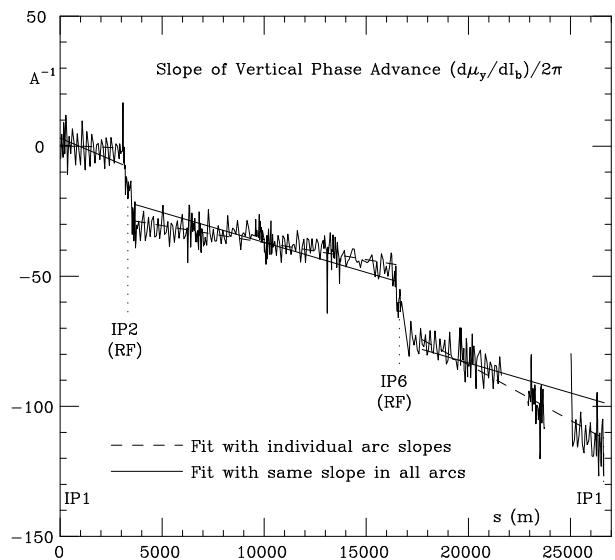
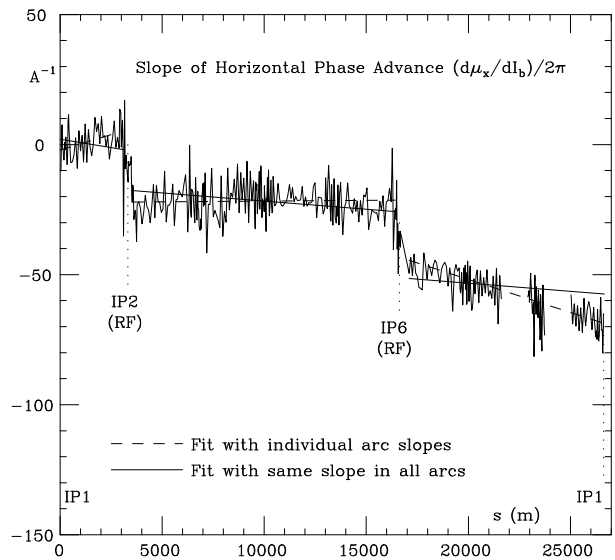


Figure 6: Dependence of phase advances on bunch current giving the reactive transverse impedance in the two planes